

Cell-to-Cell Variability in PI3K Protein Level Regulates PI3K-AKT Pathway Activity in Cell Populations

Tina L. Yuan,^{1,3,5} Gerburg Wulf,^{2,4} Laura Burga,^{2,4} and Lewis C. Cantley^{1,3,*}

¹Department of Systems Biology

²Department of Medicine

Harvard Medical School, Boston, MA 02115, USA

³Division of Signal Transduction

⁴Division of Hematology and Oncology

Beth Israel Deaconess Medical Center, Boston, MA 02115, USA

Summary

Background: Cell-to-cell variability in populations has been widely observed in mammalian cells. This heterogeneity can result from random stochastic events or can be deliberately maintained through regulatory processes. In the latter case, heterogeneity should confer a selective advantage that benefits the entire population.

Results: Using multicolor flow cytometry, we have uncovered robust heterogeneity in phosphoinositide 3-kinase (PI3K) activity in MCF10A cell populations, which had been previously masked by techniques that only measure population averages. We show that AKT activity is bimodal in response to EGF stimulation and correlates with PI3K protein level, such that only cells with high PI3K protein can activate AKT. We further show that heterogeneity in PI3K protein levels is invariably maintained in cell populations through a degradation/resynthesis cycle that can be regulated by cell density.

Conclusions: Given that the PI3K pathway is one of the most frequently upregulated pathways in cancer, we propose that heterogeneity in PI3K activity is beneficial to normal tissues by restricting PI3K activation to only a subset of cells. This may serve to protect the population as a whole from overactivating the pathway, which can lead to cellular senescence or cancer. Consistent with this, we show that oncogenic mutations in p110 α (H1047R and E545K) partially evade this negative regulation, resulting in increased AKT activity in the population.

Introduction

Among the thousands of proteins expressed in a single cell at any one time, it is inevitable that even genetically identical cells will have variable expression of certain proteins. This cell-to-cell heterogeneity can have profound effects on the phenotype of a population. In bacteria and yeast, a heterogeneous population has a better chance of surviving in fluctuating environments [1–3]. In cancer cells, variable protein expression results in nonuniform responses to anticancer agents and only “fractional” killing, which is beneficial to the tumor but detrimental to the patient [4–7].

Population heterogeneity can be the result of genetic and nongenetic variability [8]. Nongenetic sources of heterogeneity

are of particular interest because they are not fixed in the population by heritable transmission. Rather, these sources can be stochastic in nature, such as random fluctuations in transcription or translation, or they can be regulated, such as through feedback mechanisms, so that variability is deliberately maintained. Flow cytometry allows us to measure protein concentrations in single cells within large populations, which has proved useful in differentiating between stochastic and regulated sources of variation. Variable protein levels caused by stochastic events are usually rare and slightly increase the coefficient of variance of an otherwise log-normal concentration distribution [9]. Regulated variance usually deviates from tight log-normal distributions and in the most extreme cases might display bimodality [10]. Additionally, variance in the expression level of these proteins tends to correlate with variance in functionally related proteins [9].

We demonstrate cell-to-cell variability in phosphoinositide 3-kinase (PI3K) pathway activation in mammary epithelial cells that is indeed bimodal and also correlates with multiple proteins in the pathway. This implies that heterogeneous PI3K activation in cell populations is maintained by a regulated process and likely confers a selective advantage. The PI3K pathway regulates numerous critical cellular functions such as proliferation, growth, and survival and is one of the most frequently altered pathways in human cancer [11]. Tumor cells have evolved numerous ways of overactivating this pathway to induce tumorigenesis, such as amplifications or mutations in upstream receptor tyrosine kinases (RTK), mutations or deletion of the negative regulator PTEN, somatic mutations in PI3K itself, and combinations of the above [12–14]. In this view, we propose that cell-to-cell variability in PI3K activity serves as a mechanism to keep overall PI3K activity limited in normal tissues to avoid hyperactivity that may lead to cancer.

Results

AKT Activation in MCF10A Populations Is Heterogeneous and Exhibits a Bimodal Distribution

To assess cell-to-cell variability in PI3K pathway activation, we acutely stimulated serum- and growth factor-starved MCF10A cells with EGF and measured AKT activity in single cells by flow cytometry. As expected, in the absence of EGF or with pretreatment with the PI3K inhibitor wortmannin, cells exhibited a log-normal distribution in the pAKT-negative gate (Figure 1A). Following treatment with saturating amounts of EGF, we observed striking heterogeneity in AKT activation characterized by the bimodal distribution of cells into the pAKT-negative (~70%) or pAKT-positive (~30%) gates (Figure 1A). The percentage of cells in the positive gate was maximal at 5–10 min and decreased over time. We found that the bimodality was not due to differential EGFR activation or total AKT protein abundance, both of which exhibit log-normal distributions and show weak correlation with pAKT status (see Figures S1A and S1B available online). Bimodality was also observed following insulin stimulation, suggesting that this is a general, rather than ligand-specific, effect on PI3K activation (Figure S1C). We also observed robust

*Correspondence: lewis_cantley@hms.harvard.edu

⁵Present address: Helen Diller Family Comprehensive Cancer Center, University of California, San Francisco, San Francisco, CA 94158, USA

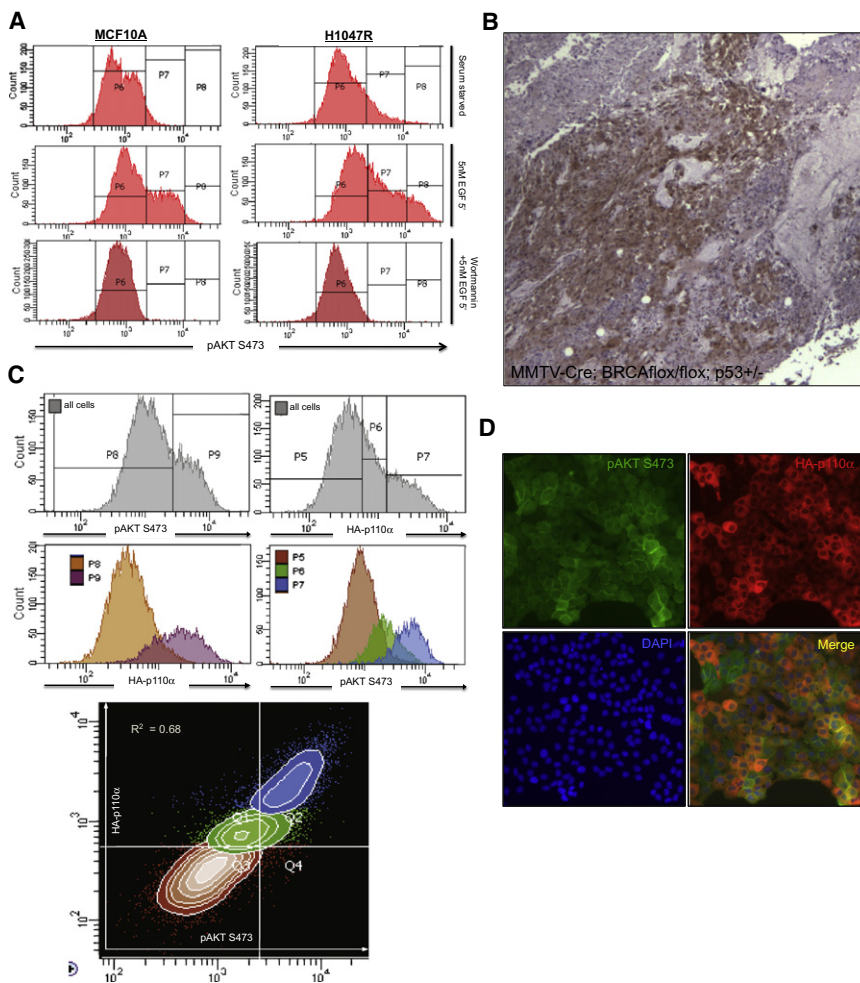


Figure 1. PI3K Pathway Activation in MCF10A Populations Is Heterogeneous

(A) Cells were starved and acutely stimulated with 5 nM EGF for 5 min with or without pretreatment with 100 nM wortmannin. Cells were then harvested and stained with anti-pAKT S473 antibody and analyzed by flow cytometry. Unstimulated and wortmannin-treated cells are pAKT negative (P6). EGF stimulation activates ~30% of cells and shifts them into the pAKT-positive gate (P7). Cells stably expressing the oncogenic H1047R p110 α mutant exhibit basal AKT activity in the unstimulated state (as previously reported), and EGF stimulation shifts more cells into the pAKT-positive gate (P7) and also increases the amplitude of pAKT signal (P8).

(B) Mammary carcinomas from MMTV-Cre; BRCA1^{flox/flox}; p53^{+/-} mice display heterogeneous pAKT positivity.

(C) MCF10A cells stably expressing HA-tagged p110 α were treated as described in (A) and costained with anti-pAKT S473 and anti-HA antibodies. HA-p110 α segregates into a bimodal distribution and correlates with pAKT status ($R^2 = 0.68$).

(D) The results from (C) were validated by immunofluorescence.

p110 α Protein Level Is Variable in Single Cells and Determines AKT Activity

Given that the bimodal AKT activation could not be explained by bimodal distribution of activated EGFR or total AKT protein, we next looked for variability in PI3K protein abundance. There are no p110 α antibodies amenable for flow cytometry, but pAKT bimodality was maintained in MCF10A cells stably

expressing HA-tagged p110 α . We thus utilized anti-HA antibodies to monitor levels of p110 α . Using single-cell analysis, we found that p110 α protein levels, like pAKT, exhibit bimodality in cell populations (Figure 1C). p110 α protein level also positively correlated with pAKT status ($R^2 = 0.68$), indicating that only cells with high levels of p110 α can activate AKT. Cells with medium levels of p110 α have intermediate levels of AKT activity, suggesting that these cells may be transitioning dynamically between the two dominant modes (Figure 1C). Subpopulations in these varying states can also be visualized by immunofluorescence (Figure 1D).

bimodal activation of AKT in another nontransformed human mammary epithelial cell line (HMEC; Figure S1E). As reported in the literature, cell populations expressing the oncogenic H1047R *PIK3CA* mutation have higher AKT activity [15–17]. The enzyme encoded by this mutant form of *PIK3CA* has been shown to have higher specific activity than that encoded by wild-type *PIK3CA* [15, 16]. To explore the possibility that this mutation shifts cells uniformly to the pAKT-positive state, we analyzed MCF10A cells stably expressing this mutant form of p110 α by flow cytometry. We observed that even in the presence of oncogenic p110 α , cells still segregate into a bimodal distribution and retain a substantial population of nonresponders. The H1047R mutation in MCF10A cells thus achieves higher average pAKT levels by shifting more cells into the pAKT-positive state (Figure 1A). This implies that the mechanism that maintains heterogeneity in cell populations is both robust and not eliminated by expression of a mutant form of PI3K with constitutively high specific activity.

Finally, we wanted to ensure that heterogeneous AKT activation is preserved in more physiological settings. Debnath et al. have previously observed sporadic pAKT staining in MCF10A 3D acinar structures, which is important for proper lumen formation [18, 19]. To see whether this heterogeneous AKT activation was observed in vivo, we analyzed spontaneously arising tumors from MMTV-Cre; BRCA1^{flox/flox}; p53^{+/-} mice and indeed observed heterogeneity in pAKT positivity (Figure 1B).

The p85 α -p110 α heterodimer is a very stable complex that does not readily dissociate, and it is thus thought that p110 α levels generally correlate with p85 α levels [20, 21]. We monitored the distribution of endogenous p85 α in MCF10A cells, and we show that levels of endogenous p85 α mirror that of HA-tagged p110 α in single cells (Figure S1D). This correlation indicates that the heterogeneity we observe is not an artifact of exogenously expressed p110 α and confirms that high levels of the entire functional holoenzyme are required for AKT activation, as expected.

p110 α Protein Levels Are Dynamic within Single Cells In agreement with previous studies [22–24], total PI3K levels do not appear to change upon growth factor stimulation, as measured by western blot (Figure 2A). To test the possibility

p110 α Protein Levels Are Dynamic within Single Cells

In agreement with previous studies [22–24], total PI3K levels do not appear to change upon growth factor stimulation, as measured by western blot (Figure 2A). To test the possibility

Heterogeneous PI3K Activation in Cell Populations

3

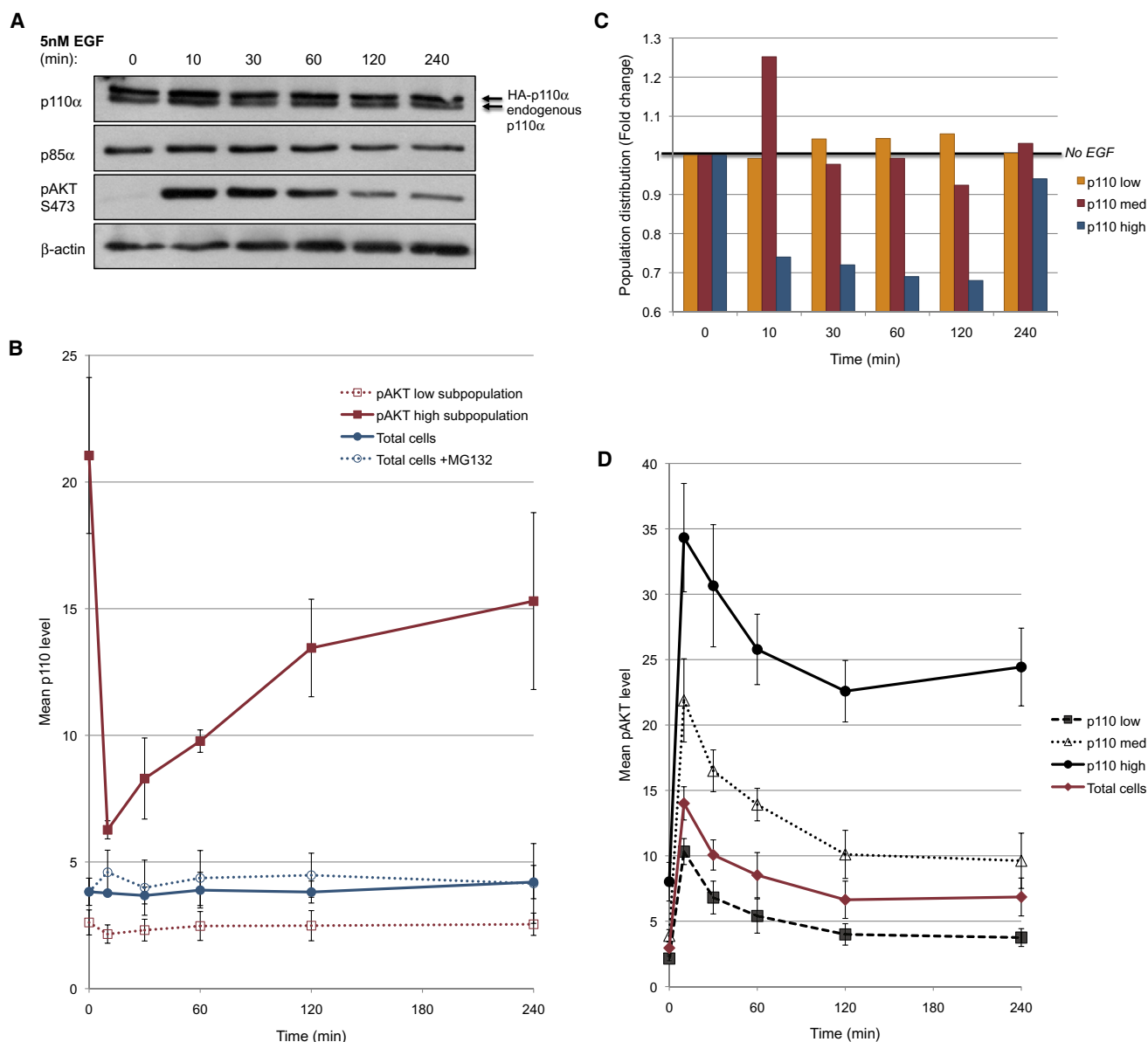


Figure 2. p110 α Levels Are Dynamic within Single Cells

(A) MCF10A cells stably expressing wild-type HA-p110 α were starved and acutely stimulated with 5 nM EGF. Cell lysates were harvested at indicated time points and analyzed by SDS-PAGE.

(B) MCF10A cells stably expressing wild-type HA-p110 α were treated as described in (A). Cells were harvested at indicated time points and analyzed by flow cytometry. The average p110 α level in the population (solid blue line) remains low and unchanging, as seen by western blot in (A). On the subpopulation level, pAKT-positive cells (solid red line) initially have high levels of p110 α , which drop precipitously at 10 min and recover over time. The pAKT-negative subpopulation (dotted red line) retains constant low levels of p110 α . The dynamic changes in p110 α levels in the pAKT-positive subpopulation can modestly influence p110 α levels of the entire population, as seen by the slight increase in p110 α in the presence of MG132 (dotted blue line).

(C) The proportion of cells in the p110 α ^{high/medium/low} gates was measured at each time point in a representative experiment described in (B). Fold change compared to time 0 is shown, indicating a shift of cells from the p110 α ^{high} to p110 α ^{medium} to p110 α ^{low} states and back. The short 4 hr time course ensures that these dynamic changes are not due to cell division.

(D) Average AKT activity was measured on the population and subpopulation levels in the cells from (B). p110 α ^{high} cells (solid black line) maximally activate AKT compared to p110 α ^{low} cells (dashed black line), which minimally activate AKT. p110 α ^{medium} cells (dotted black line) have intermediate levels of pAKT. Given that the p110 α ^{high} cells only represent ~30% of the population, the average pAKT level on the population level (red line) is only slightly higher than the p110 α ^{low} line. Data are from at least three independent experiments, and error bars represent standard error of the mean.

that p110 α protein levels are dynamic on the subpopulation level, we measured p110 α levels in pAKT-positive and pAKT-negative subpopulations over a time course of EGF stimulation by single-cell analysis. Surprisingly, we observed dynamic changes in p110 α protein in pAKT-positive cells. This minor

subgroup of cells has the highest levels of p110 α (and the highest levels of pAKT) and undergoes a precipitous drop in p110 α protein at 10 min after EGF stimulation, when AKT activity is maximal (Figure 2B). Over the next 4 hr, this population gradually recovers p110 α levels (Figure 2B). In contrast, the major

subgroup of cells with low levels of pAKT and low p110 α does not show a significant decline in p110 α (or activation of AKT) during the time course of EGF stimulation. We attempted to verify these results with live cell imaging of fluorescently tagged p110 α , but the size of the fluorescent protein-p110 fusion prohibited efficient transfection and expression.

However, our observed changes in p110 α levels also correlate with a striking change in the proportion of cells in the p110 α^{high} , p110 α^{medium} , and p110 α^{low} subpopulations over the time course of EGF stimulation. After 10 min of EGF stimulation, there is a major drop in the proportion of cells in the p110 α^{high} state and an increase in the proportion of cells in the p110 α^{medium} state (Figure 2C). Over the next 4 hr, the populations recover to the original distribution (Figure 2C). These data indicate that there is a significant decrease in p110 α levels in a subpopulation of cells characterized by high pAKT and high p110 α . The failure to detect this acute change in p110 α by western blot can be explained by the fact that this population represents only a minor fraction of total cells, whereas the protein in a western blot is dominated by a major fraction of cells (70%–80%) that fail to activate the PI3K/AKT pathway and maintain static p110 α levels. Endogenous p85 α levels exhibit nearly identical kinetics to p110 α , indicating that the entire holoenzyme is dynamically regulated to modulate AKT activity (Figure S2).

We also plotted the time course of EGF-stimulated AKT phosphorylation in the subpopulations of cells that had high, medium, or low levels of p110 α (Figure 2D). The subset of cells with the highest level of p110 α had not only the highest pAKT signal amplitude but also the longest pAKT signal duration. However, the overall population response was dominated by the major subset of cells that had minimal AKT phosphorylation.

Dynamic Changes in p110 α Protein Levels Are Regulated by a Degradation/Resynthesis Cycle

We next sought to understand the mechanism by which p110 α levels were modulated. In these cells, HA-p110 α expression is driven by the CMV promoter, suggesting that variability in p110 α expression is posttranscriptionally regulated. To test whether the drop in p110 α levels in actively signaling cells was due to proteasome-mediated degradation, we treated cells with MG132 and observed an increase in p110 α protein on the population level (Figure 3A). On the subpopulation level, MG132 treatment resulted in the accumulation of cells in the p110 α^{medium} state and a loss of cells from the p110 α^{low} state (Figure 3B). This suggests that proteasome-mediated degradation of p110 α transitions cells from the p110 $\alpha^{\text{high/medium}}$ state to the p110 α^{low} state, thereby negatively regulating AKT activity. Short-term treatment of cells with MG132 prior to acute EGF stimulation partially rescues the drop in p110 levels in pAKT high cells and prevents the shift of cells from the p110 α^{high} to p110 α^{medium} state (Figures S3A and S3B).

To show that p110 α can be resynthesized and thus transition cells from the p110 α^{low} to the p110 $\alpha^{\text{medium/high}}$ state, we treated cells with cyclohexamide (CHX). On the population level, we observed an overall decrease in p110 α protein with CHX treatment (Figure 3A). On the subpopulation level, we observed an accumulation of cells in the p110 α^{low} state with concomitant loss of cells from the p110 α^{medium} and p110 α^{high} states (Figure 3B). These data show that p110 α resynthesis is responsible for shifting cells from the p110 α^{low} state to the p110 α^{high} state, thereby generating cells competent to activate AKT.

Our results thus far suggest a model whereby p110 α levels in single cells oscillate via a degradation/resynthesis cycle, which transitions cells through phases of high p110 α (competent to activate the pathway) and low p110 α (incompetent to activate the pathway). Large populations contain cells in various stages of this cycle, thus accounting for the vast heterogeneity we observe (Figure 3C). Though many extrinsic factors are likely to influence the duration and progression of this cycle, we found no correlation between p110 α or pAKT status with cell cycle, as assessed by DNA content, or with cell size or granularity (Table S1 and Figure S3C).

Hot Spot *PIK3CA* Mutations Confer Stabilization of the p110 α^{high} State

Escaping this negative regulation of AKT may be particularly important in cancer cells, given that H1047R-expressing MCF10A cells and several tumor-derived breast cancer cell lines can activate AKT in a greater proportion of cells compared to nontransformed cell lines (Figure 1A; Figure S1E). To test whether this was due to the ability to stabilize the p110 α^{high} state, we measured the level of p110 α in MCF10A cells stably expressing exogenous HA-tagged wild-type, H1047R mutant, or E545K mutant p110 α .

Both mutant forms of p110 α were expressed at higher levels than wild-type p110 α (Figure 4A), which was due to the maintenance of more cells in the p110 α^{high} state and fewer cells in the p110 α^{low} state (Figures 4B, 4C, and 4H). To ensure that these differences were not due to variability in retroviral infection efficiency, we tested multiple batches of cell lines, and all lines were grown under selection for several generations before use in experiments.

We next sought to determine whether the mutant forms of p110 α were stabilizing the p110 α^{high} state by resisting degradation. We monitored the degradation kinetics of the mutant cell lines as we did in Figure 2B. Though both mutant cell lines underwent rapid p110 α degradation following EGF stimulation, the E545K mutant displayed more muted degradation (though this was, in part, due to higher basal expression), and both mutants exhibited considerable variability between experiments compared to wild-type (Figure 4D). Additionally, MG132 treatment of asynchronously growing mutant cells did not result in an increase in overall p110 α levels, as observed in the wild-type line (Figure 4E). These results suggest that the H1047R and E545K mutations confer resistance to proteasome-mediated degradation under exponential growth conditions that may be distinct from the acute degradation that occurs following EGF stimulation of starved cells. Notably, all cell lines responded similarly upon CHX treatment, ruling out the possibility that mutant p110 α is preferentially synthesized (Figure 4E).

To determine whether stabilization of PI3K contributes to the oncogenic potential of the mutants, we compared overall AKT activity to total p110 α levels in mutant and wild-type cells. During exponential growth, H1047R- and E545K-expressing cells had 3.9-fold and 2.4-fold, respectively, more total AKT activity than those expressing wild-type *PIK3CA*, though the corresponding p110 α levels were only 2.0-fold and 1.7-fold higher (Figures 4A, 4F, and 4G). Given that these mutant forms of p110 α are more enzymatically active [15, 16], we predict that the combination of more cells in the p110 α^{high} state and higher enzymatic activity cooperate to induce oncogenic levels of AKT activity.

Heterogeneous PI3K Activation in Cell Populations

5

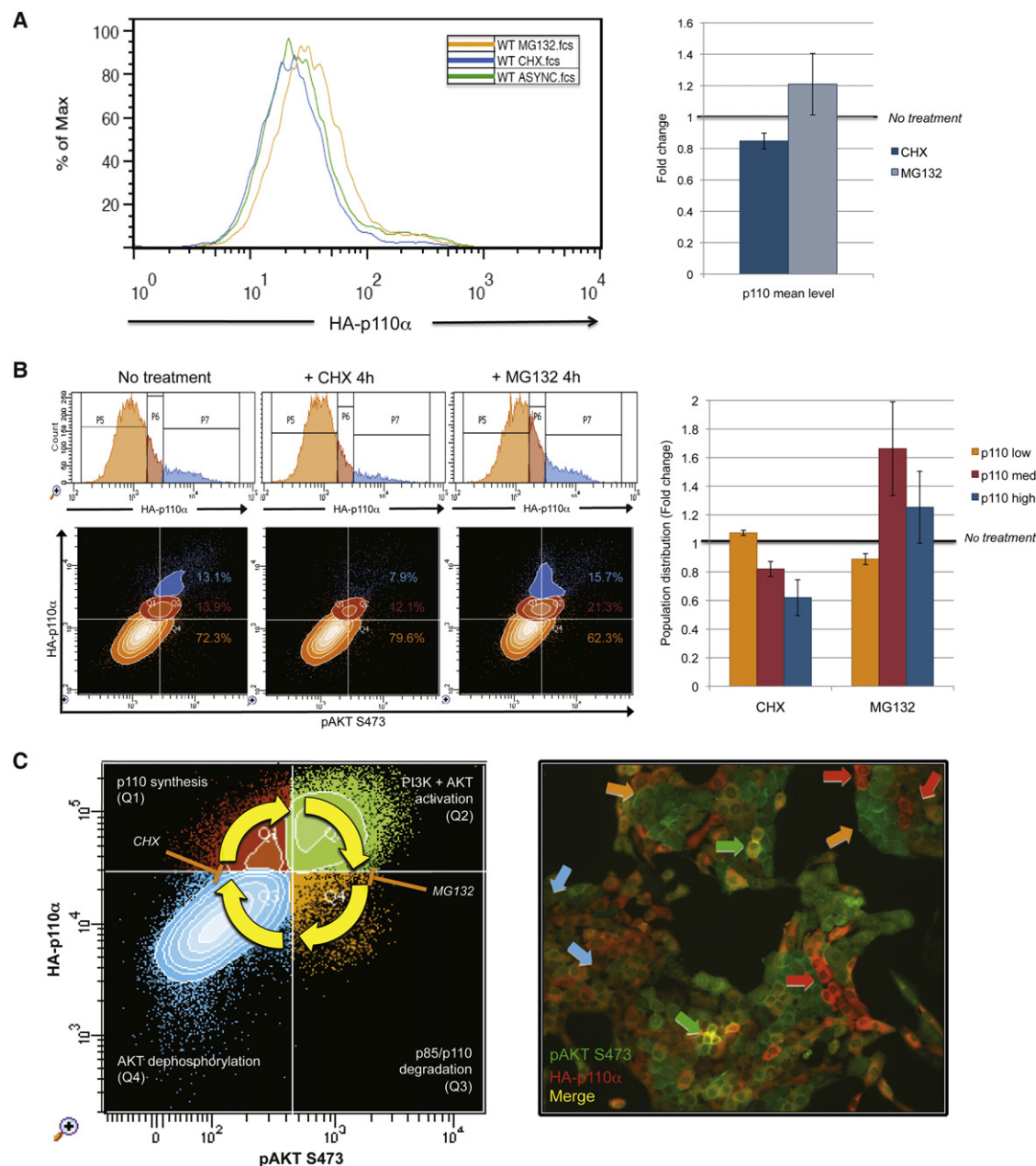


Figure 3. Changes in p110 α Levels Are Regulated by a Degradation/Resynthesis Cycle

(A) Asynchronously growing MCF10A cells expressing wild-type HA-p110 α were treated for 4 hr with 100 μ g/mL cyclohexamide (CHX) or 20 μ M MG132 and analyzed by flow cytometry. Left: on the population level, CHX (blue line) and MG132 (orange line) treatment shifted the p110 α distribution to the left and right, respectively, compared to untreated cells (green line). Right: these shifts in p110 α levels correlate with changes in overall pAKT level.

(B) On the subpopulation level, CHX treatment inhibits the accumulation of cells in the p110 α ^{medium/high} gates by retaining cells in the p110 α ^{low} state. MG132 treatment results in the accumulation of cells in the p110 α ^{medium/high} gates. Changes in population distribution are quantified in the right panel. Data are from at least three independent experiments, and error bars represent standard error of the mean.

(C) Model of PI3K degradation/resynthesis cycle that regulates pathway activation. Left: inactive cells are p110 α ^{low}; pAKT^{low} (Q4). Extrinsic signals trigger de novo synthesis of PI3K protein, transitioning cells to a p110 α ^{high}; pAKT^{low} state (Q1), where they are competent to activate the pathway. Once a growth signal is received, cells transition to the p110 α ^{high}; pAKT^{high} state (Q2), and the PI3K pathway is fully activated. Shortly after activation, PI3K is rapidly degraded and cells enter the p110 α ^{low}; pAKT^{high} state (Q3). Once AKT is fully dephosphorylated, cells return to the inactive (Q4) state. Right: immunofluorescence of EGF-stimulated cells shows cells in each of these four stages of the cycle.

p110 α ^{high} Cells Initiate Colony Formation

We next investigated whether p110 α ^{high} cells had unique functional roles. We seeded single cells from wild-type, H1047R, and E545K parental cell lines and generated clonal cell lines. Remarkably, nearly 100% of the clones that emerged exhibited

a bimodal profile that was the reverse of the parental population. At early passage, the majority of cells were in the p110 α ^{high} state, and a minority was in the p110 α ^{low} state, with corresponding changes in pAKT (Figure 5A and Table S2). These results suggest that only p110 α ^{high} cells were

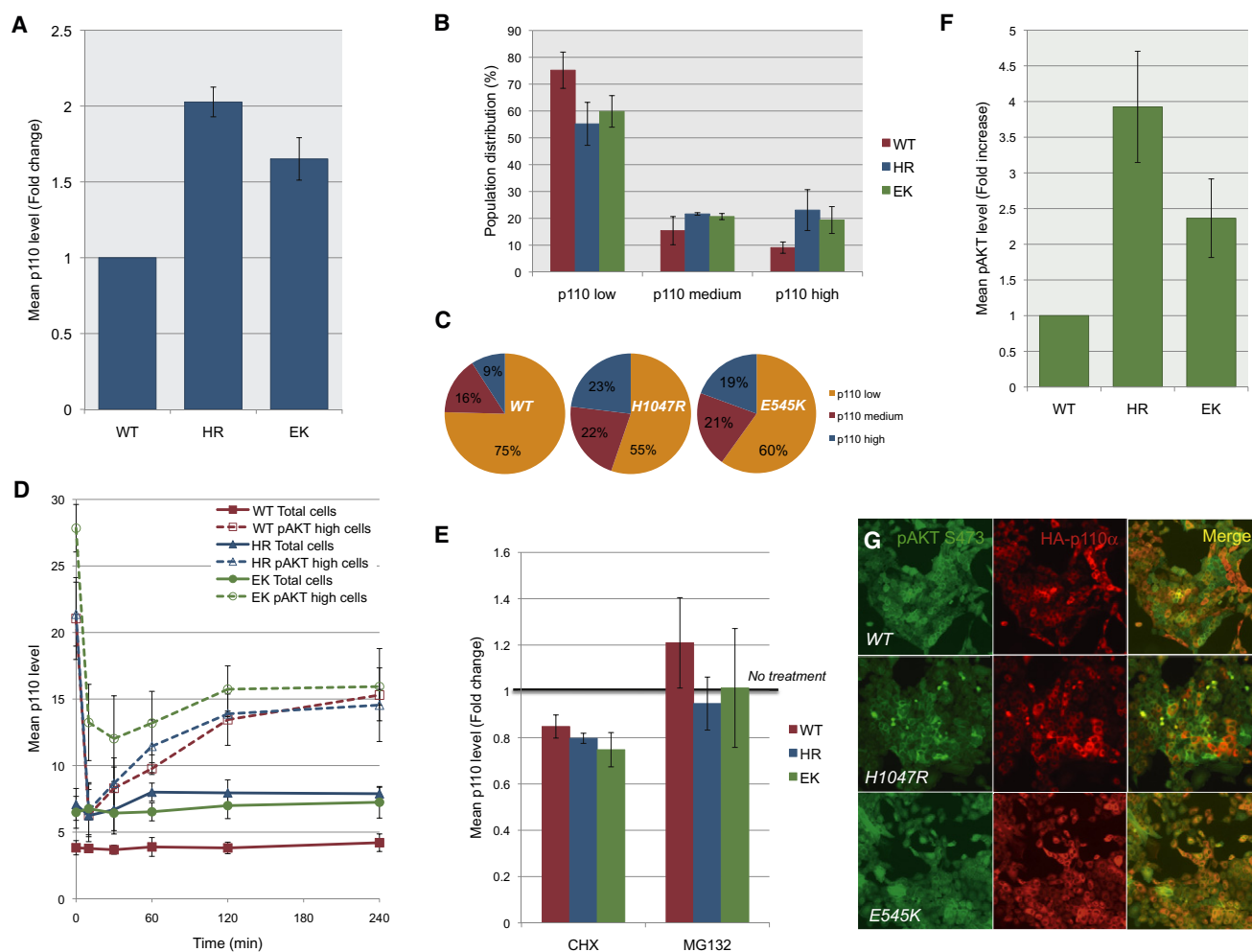


Figure 4. *PIK3CA* Mutations Stabilize the $p110\alpha^{\text{high}}$ State

(A) Asynchronously growing MCF10A cells stably expressing HA-tagged wild-type or mutant $p110\alpha$ (H1047R or E545K) were analyzed by flow cytometry. Cells expressing the H1047R or E545K mutations had 2.0-fold and 1.7-fold, respectively, higher levels of $p110\alpha$ compared to wild-type. (B) The proportion of cells within the $p110\alpha^{\text{high/medium/low}}$ gates was measured for the three cell lines. Both mutant cell lines had more cells with high levels of $p110\alpha$ and fewer cells with low levels of $p110\alpha$. (C) Asynchronously growing cells expressing wild-type $p110\alpha$ only have ~25% of cells actively signaling or primed to activate signaling compared to >40% in either mutant cell line. Numbers represent an average of three experiments. (D) Cells expressing wild-type or mutant $p110\alpha$ were treated as described in Figure 2B. Total levels of $p110\alpha$ in the whole population did not change over time (solid lines), though the mutant cells retained higher average $p110\alpha$ levels than the wild-type cells. In the $pAKT^{\text{high}}$ subpopulations (dashed lines), the mutants followed similar dynamic changes in $p110\alpha$ levels as described for wild-type, though with much greater variability. (E) Asynchronously growing wild-type and mutant lines were treated with CHX or MG132 as described in Figure 3A. All cell lines showed a decrease in $p110\alpha$ levels following treatment with CHX. However, the mutant lines were less sensitive to the MG132 treatment than the wild-type line. (F) Average AKT activity in asynchronously growing wild-type and mutant cell populations was measured by flow cytometry. The H1047R and E545K mutant lines exhibited 3.9-fold and 2.4-fold increases, respectively, in total pAKT level compared to wild-type. Data are from at least three independent experiments, and error bars represent standard error of the mean. (G) Wild-type and mutant cells were analyzed by immunofluorescence, as described in Figure 1.

capable of forming colonies, at least partially by maintaining high AKT activity. This is likely important for overcoming low cell-density-related and replicative stresses, because we observed that cell lines overexpressing $p110\alpha$, either wild-type or mutant, survived many more serial passages than clones with only endogenous levels of $p110\alpha$ (Figure 5B and Table S2).

If enrichment for $p110\alpha^{\text{high}}$ cells is important in the early stages of colony formation, we next wanted to test whether the clones reverted back to the parental distribution once the population established steady exponential growth. We compared $p110\alpha$ levels at early and late passages and indeed

saw reversion to the parental distribution with the majority of cells in the $p110\alpha^{\text{low}}$ state in late passages (Figure 5C). We carefully monitored the rate of reversion by measuring $p110\alpha$ levels in sequential passages and observed a gradual decrease in the percentage of cells with high $p110\alpha$ in nearly all clones by passage 8 (Figure 5D). This suggests that $p110\alpha^{\text{high}}$ cells are critical for colony formation and early clonal expansion, but heterogeneous populations of predominantly $p110\alpha^{\text{low}}$ cells facilitate exponential growth. To ensure that there was no genetic component to these effects, we established a second generation of clones from primary clonal populations and observed the same trends (Table S2).

Heterogeneous PI3K Activation in Cell Populations

7

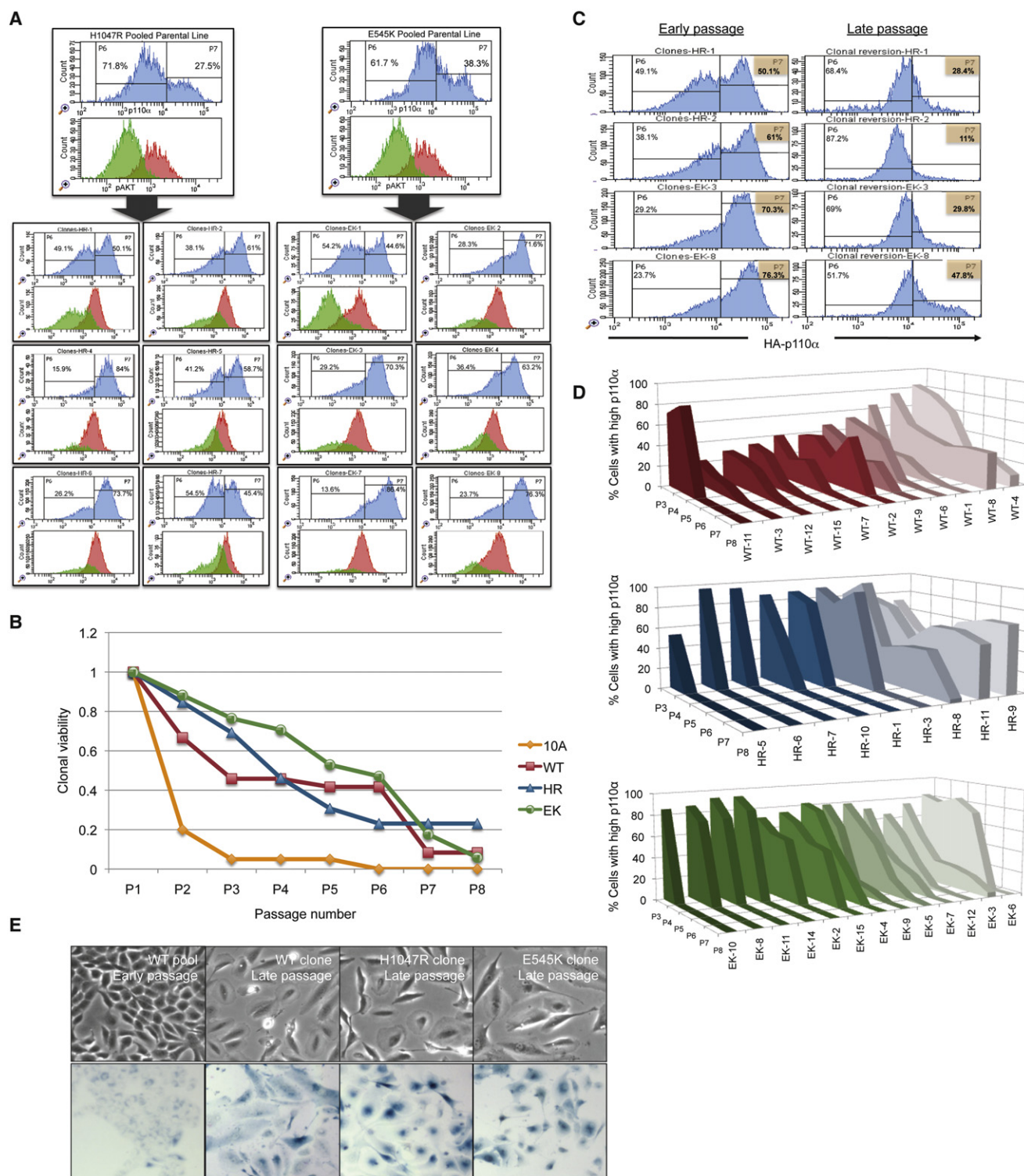


Figure 5. Cells with High Levels of p110α Are Important for Colony Formation

(A) On passage 3, clonal cell lines were starved, acutely stimulated with 5 nM EGF, and analyzed by flow cytometry. In each set of histograms, the top (blue) measures p110α and the bottom measures pAKT S473 of p110α^{low} (green) and p110α^{high} (red) cells.

(B) Clones overexpressing wild-type or mutant p110α survived more passages than cells with only endogenous levels of p110α. Additionally, expression of either mutant form of p110α increased clonal viability at early passages compared to expression of wild-type p110α.

(C) Clones at late passage (>10) were analyzed as described in (A) and invariably reverted to the parental bimodal distribution characterized by a large p110α^{low} subpopulation and a small p110α^{high} subpopulation.

(D) To monitor the rate of reversion, we measured the percent of cells with high levels of p110α by flow cytometry for six serial passages. Mutant clones (middle and bottom) achieved higher p110α^{high} percentages and reverted more slowly than wild-type clones (top). Notably, many mutant clones (HR-5,6,7 and EK-10,8,11,14) failed to revert and instead ceased proliferating at early passage.

(E) Clones that stopped growing stained positively for senescence-associated β-galactosidase activity compared to an exponentially growing control line.

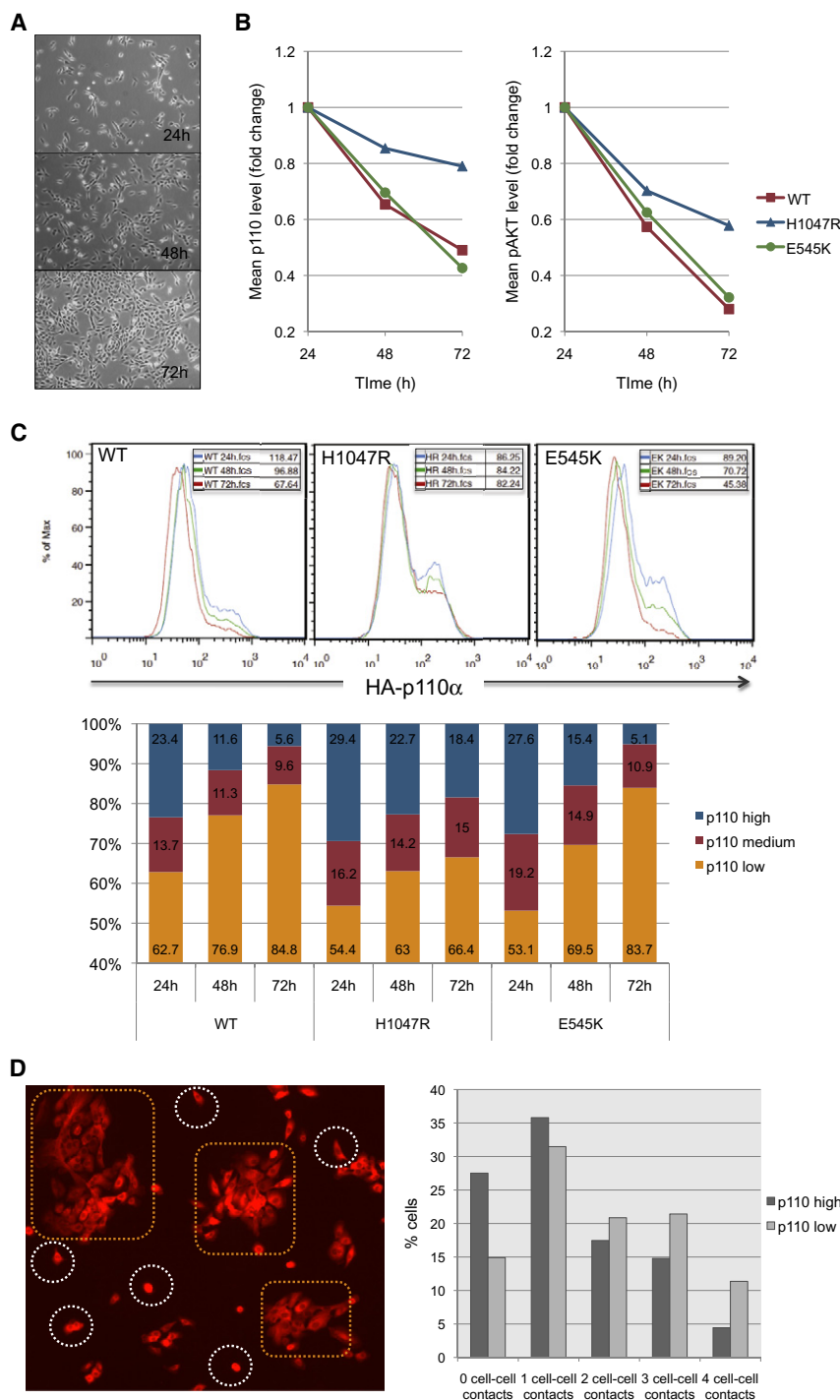


Figure 6. Establishing Cell-Cell Contacts Stabilizes the $p110\alpha^{\text{low}}$ State

(A) Cells achieve ~ 1.5 doublings every 24 hr, thereby increasing the number of cell-cell contacts.

(B) Asynchronously growing cells were harvested every 24 hr and analyzed by flow cytometry. As cell density increases, average $p110\alpha$ (left) and $pAKT$ (right) levels in the population decrease. Data shown are from one representative experiment.

(C) Analyzed on the subpopulation level, the decrease in $p110\alpha$ can be attributed specifically to a decrease in the $p110\alpha^{\text{high}}$ subpopulation and an accumulation of the $p110\alpha^{\text{low}}$ subpopulation.

(D) To verify these results, we grew cells to $\sim 50\%$ confluency and assessed $p110\alpha$ levels by immunofluorescence (left). Cells with few or no cell-cell contacts (white circles) stained brightly for HA- $p110\alpha$, whereas cell clusters with many cell-cell contacts (orange boxes) displayed heterogeneity in HA- $p110\alpha$ staining intensity. The number of cell-cell contacts was counted for 875 individual cells and compared to their $p110\alpha$ status (right). $p110\alpha^{\text{high}}$ cells were enriched for cells with 0–1 cell-cell contacts, and $p110\alpha^{\text{low}}$ cells were enriched for cells with 2–4 cell-cell contacts.

Importantly, the few clones that failed to undergo a reversion to the parental distribution were predominantly mutant clones with very high percentages of $p110\alpha^{\text{high}}$ cells (Figure 5D). These clones ceased to proliferate after passage 3–4 and exhibited a spindly morphology and senescence-associated β -galactosidase activity (Figure 5E). We find these data to be consistent with a model in which reversion to a bimodal distribution of primarily $p110\alpha^{\text{low}}$ cells is required to maintain exponential growth and in which failure to revert results in oncogene-induced senescence.

Establishing Cell-Cell Contacts Stabilizes the $p110\alpha^{\text{low}}$ State

If low cell density contributed to the induction of high $p110\alpha$ during colony formation, we wanted to explore the possibility that increasing cell-cell contacts induces the $p110\alpha^{\text{low}}$ state. We measured $p110\alpha$ levels of exponentially growing populations every 24 hr and found that $p110\alpha$ and $pAKT$ levels steadily decreased as cell density

increased (Figures 6A and 6B). The decrease in total $p110\alpha$ can be attributed specifically to a drop in the proportion of $p110\alpha^{\text{high}}$ cells and an accumulation of $p110\alpha^{\text{low}}$ cells (Figure 6C). This is also apparent in small cell clusters, where $p110\alpha$ levels are heterogeneous compared to lone cells that tend to be $p110\alpha^{\text{high}}$ (Figure 6D). Under these low-density growth conditions, the $p110\alpha^{\text{high}}$ population is enriched for cells with 0–1 cell-cell contacts, whereas the $p110\alpha^{\text{low}}$ population is enriched for cells with 2–4 cell-cell contacts (Figure 6D).

Additionally, reverted clonal cell lines exhibited similar $p110\alpha$ kinetics after EGF stimulation to parental populations (Figures S4A–S4C). Interestingly, at passage 3, both H1047R- and E545K-derived clones harbored higher percentages of $p110\alpha^{\text{high}}$ cells compared to wild-type clones and reverted to the parental distribution at a slower rate than wild-type (Figure 5D). This is consistent with our previous observation that mutant $p110\alpha$ can stabilize the $p110\alpha^{\text{high}}$ state (Figure 4; Figure S4D).

increased (Figures 6A and 6B). The decrease in total $p110\alpha$ can be attributed specifically to a drop in the proportion of $p110\alpha^{\text{high}}$ cells and an accumulation of $p110\alpha^{\text{low}}$ cells (Figure 6C). This is also apparent in small cell clusters, where $p110\alpha$ levels are heterogeneous compared to lone cells that tend to be $p110\alpha^{\text{high}}$ (Figure 6D). Under these low-density growth conditions, the $p110\alpha^{\text{high}}$ population is enriched for cells with 0–1 cell-cell contacts, whereas the $p110\alpha^{\text{low}}$ population is enriched for cells with 2–4 cell-cell contacts (Figure 6D).

Thus, cell-cell contacts may modulate p110 α levels in order to establish contact inhibition and/or confluence arrest.

We next considered the possibility that cells with high AKT activity are enriched at the unencumbered edges of tumors, which are less confluence inhibited and highly proliferative. These “pushing margins” are a distinct, though molecularly uncharacterized, feature of mutant *BRCA1*-driven tumors [25, 26]. We thus stained mammary tumors arising from MMTV-Cre; *BRCA1*^{flox/flox}; p53^{+/-} mice for pAKT S473. We detected heterogeneous pAKT positivity throughout the tumor (Figure S5A) and an enrichment of pAKT-positive cells along pushing margins (Figures S5B–S5F) and in the lumens of ductal hyperplasias (Figures S5G and S5H). Both of these regions represent areas with fewer cell-cell contacts, supporting our hypothesis that low cell density enhances the pAKT-positive state. However, given that no antibodies against p110 α or p85 α are amenable to immunohistochemical staining, we cannot confirm that this high AKT activity correlates with high PI3K protein.

Discussion

Nongenetic cell-to-cell variability has been observed in numerous cellular systems and can lead to distinct cellular fates. The most classic example is Ferrell and Machleder’s study of *Xenopus* oocyte maturation, which shows that variability in mitogen-activated protein kinase phosphorylation leads to either a G2 or metaphase arrest [27]. Similarly, high or low levels of Nanog determine the potential of embryonic stem cells to terminally differentiate [10, 28], and high or low levels of Sca-1 dictate the proclivity for hemapotoietic progenitor cells to commit to the erythroid or the myeloid lineage [29]. Another cellular fate that is determined by variable protein expression is the drug-tolerant/drug-sensitive state. In certain cell lines, gefitinib resistance can be conferred by high IGF-1R signaling and high KDM5A expression [7], and camptothecin resistance can be conferred by high DDX5 or RFC1 expression [4]. Our study now shows that heterogeneity in signal transduction is another meaningful source of cell-to-cell variability that does not result in distinct cell fates, but rather influences the transient behavior of the entire population.

We show that a bimodal distribution of AKT activation is an invariable characteristic of exponentially growing MCF10A cells. We propose that limiting AKT activity to only 20%–30% of cells in a population serves two related purposes: (1) to prevent senescence, and (2) to maintain suboncogenic levels of PI3K activity in large populations.

Our data show that clonal populations that are unable to revert to the parental distribution of primarily p110 α ^{low} cells undergo cellular senescence. In these clones, p110 α ^{high}; pAKT^{high} cells comprise 80%–90% of the population immediately prior to senescence, indicating that such high PI3K activity is not sustainable. These results are consistent with models of p53-dependent cellular senescence associated with the loss of two negative regulators of PI3K, PTEN and inositol polyphosphate 4-phosphatase type II (INPP4B) [30, 31]. Given that MCF10A cells are p53 replete, it is possible that overaccumulation of p110 α ^{high} cells induces senescence by the same mechanism.

A second selective advantage of maintaining variability in PI3K activity may be to maintain suboncogenic levels of PI3K activity in large populations such as tissues and organs. Given that overactivation of this pathway is one of the most frequent

events in cancer, permitting PI3K activation in only a fraction of cells within a population may be a simple mechanism to limit overall PI3K activity. However, we show that variability is not completely overcome in populations expressing oncogenic forms of p110 α or in epithelial tumor sections, which may have important implications on tumor susceptibility to PI3K inhibitors.

Assuming that only tumor cells with high levels of pathway activation are likely to die in response to acute inhibition of PI3K, then tumors with mosaic patterns of pathway activation (e.g., as judged by pAKT staining) will exhibit only a partial response to a PI3K (or AKT) inhibitor. The mosaic pattern of pathway activation could be due to genetic variability or oscillation between high and low levels of PI3K expression (as seen in MCF10A cells). In the latter case, it may be possible to kill a larger fraction of the tumor cells by adjusting the therapy to ensure that the subset of cells that are protected from PI3K inhibitor therapy at the time of the initial dose become exposed to the inhibitor a second time as they cycle into a high PI3K pathway state. Thus, a detailed understanding of the pharmacokinetics of the drug is important in deciding the intensity and frequency of dosing. Although continuous high doses of PI3K inhibitors over several days or weeks might effectively kill all tumor cells as they cycle into the high activity state, dose-limiting toxicities might preclude such treatment. An alternative approach of using a very high single dose once a week could avoid toxicities associated with continuous dosing and result in 20%–30% tumor cell death at the first treatment, followed by a period in which another 20%–30% of the resistant tumor cells cycle into the high PI3K pathway state and die at the second treatment and so on.

Various preclinical studies using PI3K inhibitors may support this hypothesis. Once-daily oral administration of the Novartis pan-PI3K/mTOR inhibitor, NVP-BEZ235, to tumor-bearing mice results in delayed tumor growth but rarely tumor regression. pAKT is ablated in these tumors 1–2 hr after dosing but reemerges several hours later [32–34]. Similar results were observed using the Genentech class 1A PI3K inhibitor, GDC-0941 [35, 36]. Our data would suggest that cells that were PI3K^{low};pAKT^{low} during the initial dose escaped the toxic effects of the drug and cycled to the PI3K^{high};pAKT^{high} state several hours later when concentrations of the drug decreased. The possibility that PI3K inhibitors are selectively targeting the advancing edges or “pushing margins” of tumors is also consistent with fact that these tumors are not advancing, but rather are stabilizing.

As we emphasized throughout this study, variability in PI3K activity in cell populations is a regulated process. Though the mechanism regulating PI3K degradation and resynthesis is beyond the scope of this study, it is tempting to consider inhibition of resynthesis to dampen PI3K activity in all cells. Another alternative is to inhibit the E3 ligase that targets PI3K for degradation, which may overactivate the pathway in all cells and induce cellular senescence. This “prosenescence” approach has recently shown promise in a prostate cancer xenograft model where PTEN is pharmacologically inhibited [37].

Experimental Procedures

Cell Lines and Cell Culture

MCF10A cells were obtained from the American Type Culture Collection and cultured as described by Debnath et al. [38]. Stable MCF10A cell lines expressing HA-tagged wild-type or mutant (H1047R or E545K) bovine p110 α

were generated by retroviral infection as previously described [15]. Expression of wild-type and mutant PIK3CA cDNA was driven by the exogenous CMV promoter of the JP1520 retroviral vector (J. Pearlberg). Where indicated, cells were starved in growth media without horse serum, EGF, or insulin for ~20 hr. Acute stimulation with growth factors was done by adding growth factor directly to the starvation medium.

Preparation of Cells for Flow Cytometry

A detailed description of how to prepare adherent cells for analysis by flow cytometry is provided in the [Supplemental Experimental Procedures](#). Antibodies used for flow cytometry were: anti-HA.11-488 conjugate (Covance); anti-p-AKT S473 (D9E)-488/647 conjugates, anti-total AKT-647 conjugate, anti-pEGFR Y1068 (Cell Signaling); anti-p85 α (Upstate Biotechnology); and various secondary Alexa Fluor dyes (Invitrogen). Data were analyzed with BD FACSDiva software (BD Biosciences), FlowJo software (Tree Star), and Cytobank [39].

Generation of Clonal Populations

Parental pooled populations were passaged >9 times in selection media to normalize for infection efficiency. Parental cells were trypsinized, diluted, and plated at a density of 1 cell/well. Colony formation was monitored daily, and media were changed every 3 days. Once colonies grew to a sufficient size, they were trypsinized and replated (passage 1), and serially passaged thereafter.

Immunoassays

Detailed protocols for immunofluorescence, immunoblotting, and immunohistochemistry are provided in the [Supplemental Experimental Procedures](#).

Supplemental Information

Supplemental Information includes five figures, two tables, and Supplemental Experimental Procedures and can be found with this article online at doi:10.1016/j.cub.2010.12.047.

Acknowledgments

We thank Jeffrey Engelman for providing us with the *PIK3CA* retroviral constructs and Kevin Courtney and Cyril Benes for insightful discussions. This work was funded by the Department of Defense Breast Cancer Research Program award W81XWH-08-1-0737 (to T.L.Y.), National Institutes of Health grant R01GM41890-21 (to L.C.C.), and Susan Komen Foundation grant BCTR0601030 and the Department of Defense Concept Award BC 046321 (to G.W.).

Received: June 5, 2010

Revised: October 20, 2010

Accepted: December 23, 2010

Published online: January 20, 2011

References

- Balaban, N.Q., Merrin, J., Chait, R., Kowalik, L., and Leibler, S. (2004). Bacterial persistence as a phenotypic switch. *Science* 305, 1622–1625.
- Acar, M., Mettetal, J.T., and van Oudenaarden, A. (2008). Stochastic switching as a survival strategy in fluctuating environments. *Nat. Genet.* 40, 471–475.
- Raj, A., and van Oudenaarden, A. (2008). Nature, nurture, or chance: Stochastic gene expression and its consequences. *Cell* 135, 216–226.
- Cohen, A.A., Geva-Zatorsky, N., Eden, E., Frenkel-Morgenstern, M., Issaeva, I., Sigal, A., Milo, R., Cohen-Saidon, C., Liron, Y., Kam, Z., et al. (2008). Dynamic proteomics of individual cancer cells in response to a drug. *Science* 322, 1511–1516.
- Spencer, S.L., Gaudet, S., Albeck, J.G., Burke, J.M., and Sorger, P.K. (2009). Non-genetic origins of cell-to-cell variability in TRAIL-induced apoptosis. *Nature* 459, 428–432.
- Gascoigne, K.E., and Taylor, S.S. (2008). Cancer cells display profound intra- and interline variation following prolonged exposure to antimitotic drugs. *Cancer Cell* 14, 111–122.
- Sharma, S.V., Lee, D.Y., Li, B., Quinlan, M.P., Takahashi, F., Maheswaran, S., McDermott, U., Azizian, N., Zou, L., Fischbach, M.A., et al. (2010). A chromatin-mediated reversible drug-tolerant state in cancer cell subpopulations. *Cell* 141, 69–80.
- Huang, S. (2009). Non-genetic heterogeneity of cells in development: More than just noise. *Development* 136, 3853–3862.
- Niepel, M., Spencer, S.L., and Sorger, P.K. (2009). Non-genetic cell-to-cell variability and the consequences for pharmacology. *Curr. Opin. Chem. Biol.* 13, 556–561.
- Kalmar, T., Lim, C., Hayward, P., Muñoz-Descalzo, S., Nichols, J., Garcia-Ojalvo, J., and Martinez Arias, A. (2009). Regulated fluctuations in nanog expression mediate cell fate decisions in embryonic stem cells. *PLoS Biol.* 7, e1000149.
- Cantley, L.C. (2002). The phosphoinositide 3-kinase pathway. *Science* 296, 1655–1657.
- Engelman, J.A. (2009). Targeting PI3K signalling in cancer: Opportunities, challenges and limitations. *Nat. Rev. Cancer* 9, 550–562.
- Courtney, K.D., Corcoran, R.B., and Engelman, J.A. (2010). The PI3K pathway as drug target in human cancer. *J. Clin. Oncol.* 28, 1075–1083.
- Yuan, T.L., and Cantley, L.C. (2008). PI3K pathway alterations in cancer: Variations on a theme. *Oncogene* 27, 5497–5510.
- Isakoff, S.J., Engelman, J.A., Irie, H.Y., Luo, J., Brachmann, S.M., Pearlman, R.V., Cantley, L.C., and Brugge, J.S. (2005). Breast cancer-associated PIK3CA mutations are oncogenic in mammary epithelial cells. *Cancer Res.* 65, 10992–11000.
- Kang, S., Bader, A.G., and Vogt, P.K. (2005). Phosphatidylinositol 3-kinase mutations identified in human cancer are oncogenic. *Proc. Natl. Acad. Sci. USA* 102, 802–807.
- Samuels, Y., Diaz, L.A., Jr., Schmidt-Kittler, O., Cummins, J.M., Delong, L., Cheong, I., Rago, C., Huso, D.L., Lengauer, C., Kinzler, K.W., et al. (2005). Mutant PIK3CA promotes cell growth and invasion of human cancer cells. *Cancer Cell* 7, 561–573.
- Debnath, J., Mills, K.R., Collins, N.L., Reginato, M.J., Muthuswamy, S.K., and Brugge, J.S. (2002). The role of apoptosis in creating and maintaining luminal space within normal and oncogene-expressing mammary acini. *Cell* 111, 29–40.
- Debnath, J., Walker, S.J., and Brugge, J.S. (2003). Akt activation disrupts mammary acinar architecture and enhances proliferation in an mTOR-dependent manner. *J. Cell Biol.* 163, 315–326.
- Brachmann, S.M., Ueki, K., Engelman, J.A., Kahn, R.C., and Cantley, L.C. (2005). Phosphoinositide 3-kinase catalytic subunit deletion and regulatory subunit deletion have opposite effects on insulin sensitivity in mice. *Mol. Cell Biol.* 25, 1596–1607.
- Ueki, K., Fruman, D.A., Brachmann, S.M., Tseng, Y.H., Cantley, L.C., and Kahn, C.R. (2002). Molecular balance between the regulatory and catalytic subunits of phosphoinositide 3-kinase regulates cell signaling and survival. *Mol. Cell Biol.* 22, 965–977.
- Luo, J., Field, S.J., Lee, J.Y., Engelman, J.A., and Cantley, L.C. (2005). The p85 regulatory subunit of phosphoinositide 3-kinase down-regulates IRS-1 signaling via the formation of a sequestration complex. *J. Cell Biol.* 170, 455–464.
- Taniguchi, C.M., Aleman, J.O., Ueki, K., Luo, J., Asano, T., Kaneto, H., Stephanopoulos, G., Cantley, L.C., and Kahn, C.R. (2007). The p85 α regulatory subunit of phosphoinositide 3-kinase potentiates c-Jun N-terminal kinase-mediated insulin resistance. *Mol. Cell Biol.* 27, 2830–2840.
- Ueki, K., Fruman, D.A., Yballe, C.M., Fasshauer, M., Klein, J., Asano, T., Cantley, L.C., and Kahn, C.R. (2003). Positive and negative roles of p85 α and p85 β regulatory subunits of phosphoinositide 3-kinase in insulin signaling. *J. Biol. Chem.* 278, 48453–48466.
- Lakhani, S.R., Jacquemier, J., Sloane, J.P., Gusterson, B.A., Anderson, T.J., van de Vijver, M.J., Farid, L.M., Venter, D., Antoniou, A., Storer-Isser, A., et al. (1998). Multifactorial analysis of differences between sporadic breast cancers and cancers involving BRCA1 and BRCA2 mutations. *J. Natl. Cancer Inst.* 90, 1138–1145.
- Liu, X., Holstege, H., van der Gulden, H., Treur-Mulder, M., Zevenhoven, J., Velds, A., Kerkhoven, R.M., van Vliet, M.H., Wessels, L.F., Peterse, J.L., et al. (2007). Somatic loss of BRCA1 and p53 in mice induces mammary tumors with features of human BRCA1-mutated basal-like breast cancer. *Proc. Natl. Acad. Sci. USA* 104, 12111–12116.
- Ferrell, J.E., Jr., and Machleder, E.M. (1998). The biochemical basis of an all-or-none cell fate switch in *Xenopus* oocytes. *Science* 280, 895–898.
- Chambers, I., Silva, J., Colby, D., Nichols, J., Nijmeijer, B., Robertson, M., Vrana, J., Jones, K., Grotewold, L., and Smith, A. (2007). Nanog safeguards pluripotency and mediates germline development. *Nature* 450, 1230–1234.

Heterogeneous PI3K Activation in Cell Populations

11

29. Chang, H.H., Hemberg, M., Barahona, M., Ingber, D.E., and Huang, S. (2008). Transcriptome-wide noise controls lineage choice in mammalian progenitor cells. *Nature* 453, 544–547.
30. Chen, Z., Trotman, L.C., Shaffer, D., Lin, H.K., Dotan, Z.A., Niki, M., Koutcher, J.A., Scher, H.I., Ludwig, T., Gerald, W., et al. (2005). Crucial role of p53-dependent cellular senescence in suppression of Pten-deficient tumorigenesis. *Nature* 436, 725–730.
31. Gewinner, C., Wang, Z.C., Richardson, A., Teruya-Feldstein, J., Etemadmoghadam, D., Bowtell, D., Barretina, J., Lin, W.M., Rameh, L., Salmena, L., et al. (2009). Evidence that inositol polyphosphate 4-phosphatase type II is a tumor suppressor that inhibits PI3K signaling. *Cancer Cell* 16, 115–125.
32. Maira, S.M., Stauffer, F., Brueggen, J., Furet, P., Schnell, C., Fritsch, C., Brachmann, S., Chène, P., De Pover, A., Schoemaker, K., et al. (2008). Identification and characterization of NVP-BEZ235, a new orally available dual phosphatidylinositol 3-kinase/mammalian target of rapamycin inhibitor with potent in vivo antitumor activity. *Mol. Cancer Ther.* 7, 1851–1863.
33. Cao, P., Maira, S.M., García-Echeverría, C., and Hedley, D.W. (2009). Activity of a novel, dual PI3-kinase/mTOR inhibitor NVP-BEZ235 against primary human pancreatic cancers grown as orthotopic xenografts. *Br. J. Cancer* 100, 1267–1276.
34. Liu, T.J., Koul, D., LaFortune, T., Tiao, N., Shen, R.J., Maira, S.M., García-Echeverría, C., and Yung, W.K. (2009). NVP-BEZ235, a novel dual phosphatidylinositol 3-kinase/mammalian target of rapamycin inhibitor, elicits multifaceted antitumor activities in human gliomas. *Mol. Cancer Ther.* 8, 2204–2210.
35. Edgar, K.A., Wallin, J.J., Berry, M., Lee, L.B., Prior, W.W., Sampath, D., Friedman, L.S., and Belvin, M. (2010). Isoform-specific phosphoinositide 3-kinase inhibitors exert distinct effects in solid tumors. *Cancer Res.* 70, 1164–1172.
36. Raynaud, F.I., Eccles, S.A., Patel, S., Alix, S., Box, G., Chuckowree, I., Folkes, A., Gowan, S., De Haven Brandon, A., Di Stefano, F., et al. (2009). Biological properties of potent inhibitors of class I phosphatidylinositol 3-kinases: From PI-103 through PI-540, PI-620 to the oral agent GDC-0941. *Mol. Cancer Ther.* 8, 1725–1738.
37. Alimonti, A., Nardella, C., Chen, Z., Clohessy, J.G., Carracedo, A., Trotman, L.C., Cheng, K., Varmeh, S., Kozma, S.C., Thomas, G., et al. (2010). A novel type of cellular senescence that can be enhanced in mouse models and human tumor xenografts to suppress prostate tumorigenesis. *J. Clin. Invest.* 120, 681–693.
38. Debnath, J., Muthuswamy, S.K., and Brugge, J.S. (2003). Morphogenesis and oncogenesis of MCF-10A mammary epithelial acini grown in three-dimensional basement membrane cultures. *Methods* 30, 256–268.
39. Kotecha, N., Krutzik, P.O., and Irish, J.M. (2010). Web-based analysis and publication of flow cytometry experiments. *Curr. Protoc. Cytom. Chapter 10*, t10, 17.